The Journal of Physical Chemistry

 VOLUME 100, NUMBER 30, JULY 25, 1996

LETTERS

Electrodeposition of Cu Nanoparticles on Decanethiol-Covered Au(111) Surfaces: An in Situ STM Investigation

Scott E. Gilbert, Ornella Cavalleri, and Klaus Kern*

Institut de Physique Expérimentale, Ecole Polytechnique Fédérale de Lausanne, CH-1015 Lausanne, Switzerland

Received: January 2, 1996; In Final Form: April 1, 1996[⊗]

Copper electrodeposition has been followed by in situ electrochemical STM on Au(111) electrodes covered by complete decanethiol monolayers. It has been found that Cu nanoparticles (2−5 nm) were formed at potentials comprising the underpotential deposition (UPD) region on clean gold. The nanoparticle clusters appear to follow a nucleation and sudden growth process as their maximal size is attained instantaneously on the time scale of the STM imaging process. Nanoparticle heights correspond to one atomic layer of Cu. The distribution density of the Cu deposits reaches a maximal value at potentials within the UPD window, as no new formation of clusters nor growth of already existing clusters is seen at potentials well into the bulk deposition potential region. Bulk deposition of isolated Cu nodules is finally seen at potentials 200 mV negative of the Nernstian potential for Cu reduction, probably resulting from thiol film breakdown. Moreover, nanoparticles remain on the Au surface at potentials as high as 1000 mV positive of the equilibrium potential. Passivation of the nanoparticles is proposed to explain these observations.

In recent years, organic self-assembled monolayers (SAMs) have been investigated for their capabilities to modify metal electrode surfaces in such a way as to create chemically and structurally well-defined and controlled electrochemical interfaces. Such modified interfaces can facilitate fundamental studies on interfacial charge transfer and produce highly selective electrocatalytic surfaces.[1] Another aspect as yet not exploited is the modification of electrocrystallization of metals on metallic electrodes for the purposes of organizing the growth in predetermined patterns. In this manner, nanostructures can be electrochemically grown directly on the metal electrode surface or as an overlayer on top of the intervening organic film. This might constitute an interesting alternative to the self-organized nanostructure growth in vacuum depostion.[2]

Several studies have begun to address the question of producing metallic overlayers on self-assembled thiol layers on gold surfaces,[3] the main motivation being the production of model organic/metal surfaces. These studies have used vacuum deposition techniques to produce the metal overlayer and have investigated the formation of chemical bonds between the thiol molecules and the deposited metal, as well as the morphology of the combined metal/SAM structure using mainly integrating techniques. In the present investigation, electrochemical deposition was chosen as it can be followed in-situ with integrating techniques (voltammetry), as well as local atomic scale probes (STM) and, second, the growth and morphology of the electrodeposited metal might be more controllable than vacuum deposition as the electrochemical potential contributes an additional parameter.

The system chosen and described herein is Cu/(decanethiol covered)Au(111). This system has been chosen because Cu deposition on Au single-crystal electrodes have been extensively studied; hence, a significant database exists that can serve as a

[⊗] Abstract published in *Advance ACS Abstracts,* June 15, 1996.

S0022-3654(96)00053-6 CCC: $12.00

means of comparison. Regarding these studies, underpotential deposition (UPD) of Cu on atomically clean and well-characterized single-crystal Au surfaces has been followed with in situ STM.[4−10] Further in situ investigations have been made on the bulk deposition of Cu on single-crystal Au in the absence[11] and presence[12−15] of organic additives which essentially modify the 3-dimensional growth of bulk deposited Cu. It has been found that the organic additives chosen for these studies act as surfactants and block surface sites on the nascent Cu nuclei where Cu atoms normally would attach and build up the bulk lattice. There is also some evidence that gold substrate surface sites are blocked by these surface active molecules, thus changing the underpotentially deposited monolayer structure. However, as these additive molecules do not self-assemble or form stable layers, organized structural modifications in the Cu layer growth cannot be realized with such systems.

Presented herein is a preliminary report of a comparative in situ STM study of the growth of Cu on clean Au (111) and Au(111) covered with a complete decanethiol monolayer. Our study shows a drastically different behavior in the Cu electrodeposition on the thiol-covered electrode. The most remarkable result is the homogeneous nucleation of Cu nanoparticles of narrow size distribution.

Experimental Section

Au Film Electrode Preparation. Electrodes were prepared by vacuum evaporation of 99.99% purity gold onto preheated round mica substrates about 1 cm in diameter. The evaporations were carried out at a base pressure of 2×10^{-6} Torr, at substrate temperatures of 280−300 °C. The quality of the surface was generally checked by STM to ensure crystallinity and the (111) orientation of the facets. As a rule, atomically flat terraces of ≥50 nm were routinely observed.

For substrates chosen to be unmodified electrodes, flame annealing treatments were performed. Substrates were heated in a butane or reducing (oxygen poor) hydrogen flame to red or orange heat for at least 60 s and then quenched in ethanol. Before transfer of the quenched films into Millipore water, ethanol was dried off in a stream of argon; otherwise the films had a tendency to detach from the mica. Air exposure was minimized as much as possible and kept to below 10 seconds, including the drying step. The substrates were then transferred with a drop of electrolyte to protect them from direct air exposure to the STM electrochemical cell, where they were mounted while protected by electrolyte.

Substrates destined to be functionalized with the decanethiol were also subjected to the same flame annealing treatment. Quenching again was carried out in ethanol, where then the substrate was transferred immediately to the ethanolic thiol solution. No drying step was necessary in this case.

Preparation of SAMs. Decanethiol (Aldrich) was used as received to prepare 1 μM solutions in pure ethanol (Fluka puriss) purged with argon. Freshly flame annealed films were transferred into the solution as described above and left immersed for 24−48 h at room temperature.

Electrochemical STM. A Besocke type beetle STM[16] was mounted with a specially designed three-electrode single-compartment electrochemical cell made from PTFE (Teflon). The total cell volume is 1.3 mL, but about half that amount of electrolyte was used in the experiments. A Pt wire counter electrode and silver wire quasireference (AgQRE) electrode were used in conjunction with the Au film working electrode, which had an exposed surface area of 0.2 cm^2. The system was potentiostated with a PAR Model 400 EC detector, configured as a single potentiostat. Tunneling bias was applied to the tip, so the tip potential was always offset from the electrode potential by the value of the bias, which was usually maintained at 50−100 mV with respect to the substrate (grounded). Tips were made from etched Pt−Ir wire and coated with BASF's anodic electrophoretic paint ZQ84, according to the method of Schulte[17] (apply at +10 V for 2 min and then cure at 200 °C for 5 min).

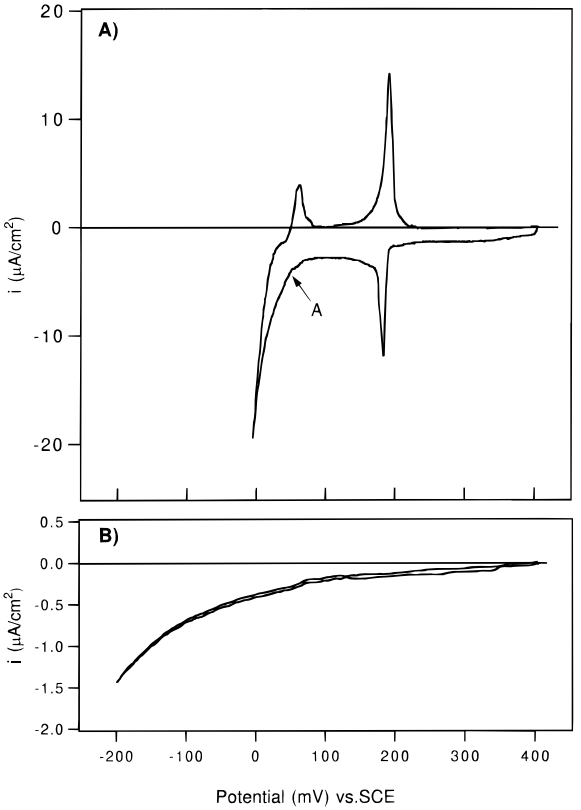

Figure 1. Cyclic voltammograms of Cu deposition on (A) bare Au(111) thin film on mica and (B) Au(111) film covered by a complete monolayer of decanethiol. The curves are shown on the same potential scale to facilitate comparison. Scan rate 5 mV/s for both voltammograms taken in nondeaerated 0.05 M H_2SO_4/1 mM $CuSO_4$. Marked point corresponds to starting potential at which STM image sequence presented in Figure 2 was acquired.

Cyclic voltammograms were taken before and after the STM measurements were made for clean gold substrates, but measurements had to be made separately for thiol-covered substrates. At least 3 h was required for thermal equilibration of the STM. Potential scales are referred to the saturated calomel reference electrode (SCE), against which the AgQRE was measured in the same electrolyte. To minimize electrolyte evaporation and aid the thermal equilibration, the STM was enclosed in a Plexiglas chamber along with a beaker of water to humidify the atmosphere. No attempt was made to exclude oxygen from the cell. Between images, the potential was stepped in 10 or 25 mV increments. As soon as the faradaic current stabilized, the image was acquired. Each potential was thus held usually for several minutes, with at about 2 min required for completion (scan frequency of 8.5 Hz) of a typical image. Again, all potentials are quoted with respect to the SCE. Tunneling conditions are stated in the figure captions.

Electrolyte Preparation. The electrolyte was chosen as that commonly used in Cu UPD studies, that is, 0.05M H_2SO_4 containing 1 mM $CuSO_4$. All glassware coming in contact with the solutions as well as the Teflon cell itself were cleaned in mixtures of H_2SO_4 and 30% H_2O_2 (70:30 by volume) prepared immediately before use.

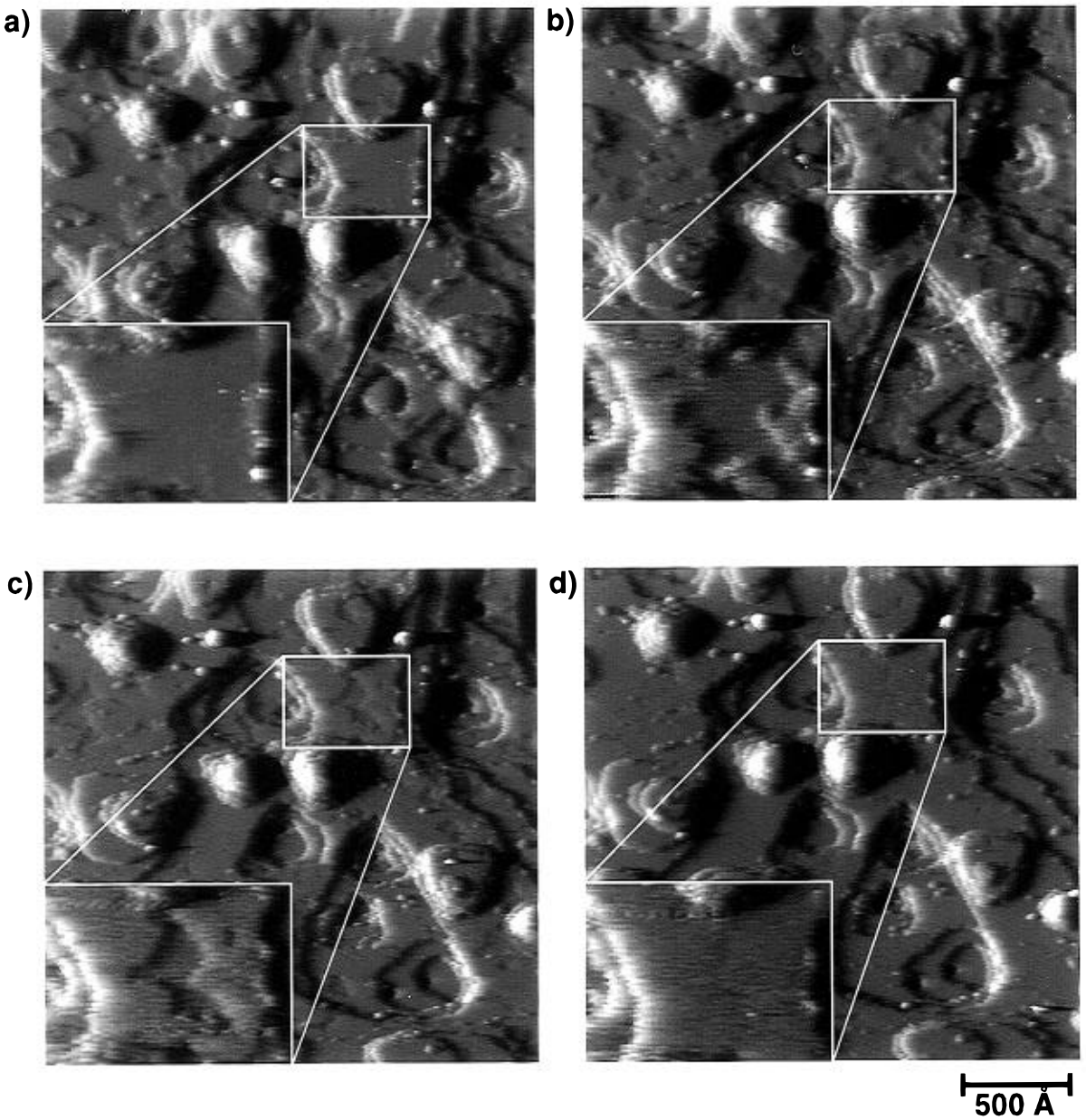

Figure 2. Image sequence of UPD of Cu on clean Au(111) surface taken at (a) 50, (b) 40, (c) 10, and (d) 0 mV (vs SCE), showing growth of (1 × 1) phase. The growth is initiated at terrace edges. Insets aid in following the growth of this phase on a terrace. Each image is 240 × 240 nm. Tunneling conditions: 0.5 nA, +50 mV tip bias.

Results and Discussion

Typical cyclic voltammograms are presented in Figure 1 for the two systems. The marked arrow points to the initial potential at which the image sequence in Figure 2 was acquired. The voltammogram in Figure 1a is representative of Cu UPD on our clean Au (111) films in the $H_2SO_4/CuSO_4$ electrolyte, although we note here that this voltammogram does not exactly reproduce all the features normally seen using bulk single-crystal Au (111) under deaerated electrolyte.[4−6] Air was not excluded from the electrolyte, and some distortion of the voltammogram due to oxygen reduction may be seen in the negative extremes. In comparison to bulk Au (111) single crystals, these films exhibit very similar Cu UPD electrochemistry. Referring to Figure 1a, the salient features are the first underpotential deposition and stripping peaks seen at +200 and +230 mV, respectively, known to represent the first 2/3 monolayer of Cu (measurement not confirmed here). A second cathodic peak at +10 mV and an associated anodic peak centered at +50 mV are the second UPD peaks, known to represent the formation of the remaining 1/3 monolayer of Cu.[7−10] Beyond 0 mV, bulk deposition of Cu begins.

In Figure 1b, a typical voltammogram is presented for a decanethiol-covered Au(111) electrode in the same electrolyte. From this we see that the film exhibits blocking behavior toward Cu deposition, as expected from results obtained with measurements on alkyl thiol-covered Au surfaces (alkyl chains with 10 or more carbon atoms) probed electrochemically.[18−21]

As a means of gaining insight into electrodeposition on these surfaces, the STM images shown in Figures 2−4 follow the evolution of the Cu deposition on both bare and thiol-covered electrodes in situ. We show in Figure 2 a series of images of a surface region of a bare electrode taken at potentials negative of the marked point shown on the CV curve in Figure 1a. These images were taken at potentials along the second UPD adsorption peak, and shown in the image sequence is the phase transition from the honeycomb-structured Cu adlattice[22,23] to the (1 × 1) psuedomorphic monolayer.[4,24,26]

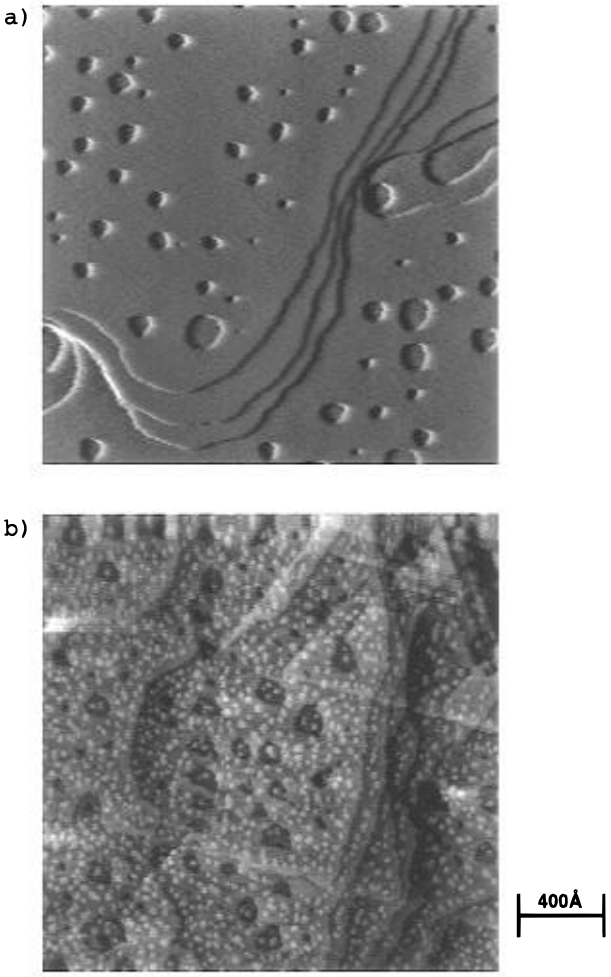

Figure 3. (a) Image of decanethiol covered Au(111) surface before immersion in electrolyte. (b) In situ image of fully developed Cu cluster distribution at +50 mV (SCE) on decanethiol-covered Au(111) surface. Note narrow size distribution. Only flat regions of terraces are decorated; no growth is seen at steps nor at hole edges. Both images are 240 × 240 nm. Tunneling conditions: 0.6 nA, +50 mV bias.

The STM images in Figure 2 depict that the phase transformation begins as patches along the upper terrace edges, and then as the potential is stepped cathodically, the islands expand inward on the terraces to coalesce with other expanding islands. Eventually, the transition is complete at 0 mV, near the threshold of bulk deposition (three-dimensional growth). We attribute the STM contrast to the presence of coadsorbed bisulfate anions, presumably inverted, and occupying positions on top of the Cu atoms in the (1 × 1) structure[26] vs their occupation of hollow sites in the honeycomb Cu adlattice, with three of the oxygen atoms bonded to neighboring Cu atoms.[22] The insets in the images aid the eye in following the growth of the (1 × 1) phase on a terrace.

Modifying the electrode surface with a monolayer of decanethiol changes the deposition process completely. This is demonstrated in Figure 3: the STM image in Figure 3a shows the morphology of the decanethiol-covered Au(111) surface before immersion into the electrolyte. Note that after thiol self-assembly, the terraces are pockmarked by holes one Au monolayer deep and approximately 10−20 nm in diameter. These are believed to either result from a corrosion process that takes place during the thiol self-assembly,[27−29] or a restructuring of the surface induced by the thiol adsorbates.[30] It is known that the bottom of the holes are also covered by thiol molecules.[27,31] These substrate defects can coalesce and finally heal out by gentle annealing between 350 and 400 K.[32]

A fully developed Cu cluster electrodeposition on the thiol-covered surface is characterized in Figure 3b. In the presence of the thiol monolayer, deposition of Cu now proceeds via homogeneous nucleation of nanosized clusters on terraces, with no preferential growth occurring at steps. Note the presence of clusters in the holes. The STM image in Figure 3b shows a typical fully developed Cu nanoparticle decoration at +50 mV on a stepped 240 × 240 nm region of the decanethiol/Au(111) sample. Thus, in the presence of the thiol modification, Cu electrodeposition now occurs by growth of seemingly randomly distributed clusters, all falling within a narrow size range.

In Figure 4, we have followed the nucleation kinetics in situ. The STM sequence depicts a patch of clusters growing across the image field. In this sequence, the images are taken approximately 0.5 h apart, and all at the same potential of +150 mV, which would correspond to compeletion of the first adsorption peak on bare gold (cf. Figure 1a). The deposition thus appears as a slowly advancing front of the growing patch of clusters, without apparent change in the clusters' positions nor sizes once formed. Although the sequence in Figure 4 is an example of what is typically observed at the incipient phase of the deposition process with thiol layers present, the kinetics of the process depends on the potential. At more negative potentials the layer can develop more quickly. Thus, the onset potential can vary with the time taken to perform the experiment. In addition, the onset potential could be influenced by the tip, which acts either by impeding the diffusion of ions or by influencing the electric field at the interface, a phenomenon which also been pointed out by Magnussen et al.[6] and explored explicitly by Li et al.[33]

Cluster formation was observed to occur by an instantaneous nucleation process. In effect, cluster formation seems to occur in patches, and it seems that cluster formation occurs abruptly in these patches. Once a threshold potential is surpassed, clusters quickly nucleate at the advancing front of the patch and quickly attain their maximum size and spatial distribution. It appears, however, that the patches spread, and new cluster nucleation occurs at the advancing front. These remain fixed throughout the remainder of the UPD range and on into the bulk deposition region of potentials.

Clusters preferentially grow on flat regions of the terraces, and almost always avoid steps or hole edges. This finding contrasts the deposition behavior of Cu on bare gold. The size distribution of the clusters remains essentially constant, with an average diameter of 3 nm and a standard deviation of more than 50%, producing a range of between 2 and 5 nm. Random samplings over the electrode surface indicate that both the size and spatial cluster distributions are virtually constant at all points. Independent of coverage, cluster heights were found to be 2−3 Å, corresponding to the height of one monolayer of Cu. We found also that the cluster positions remain fixed during scanning. However, we did not systematically vary the tip−sample distance in an attempt to dislodge them. It was found, though, that rinsing the electrode with a stream of ethanol or water after the STM experiment did not result in dislodging or removing the clusters.

The cluster size and density distributions remain surprisingly stable as the potential is taken to more cathodic values. Sweeping the potential well into the bulk deposition zone resulted in no further modification of already existing clusters but did finally result in isolated bulk deposits of Cu nodules. The sequence shown in Figure 5 bears witness to this observation, where the images in Figure 5a−d depict the growth of a bulk nodule. The image sequence begins at a potential of −210 mV, where the Cu nanoparticle decoration seen on this portion

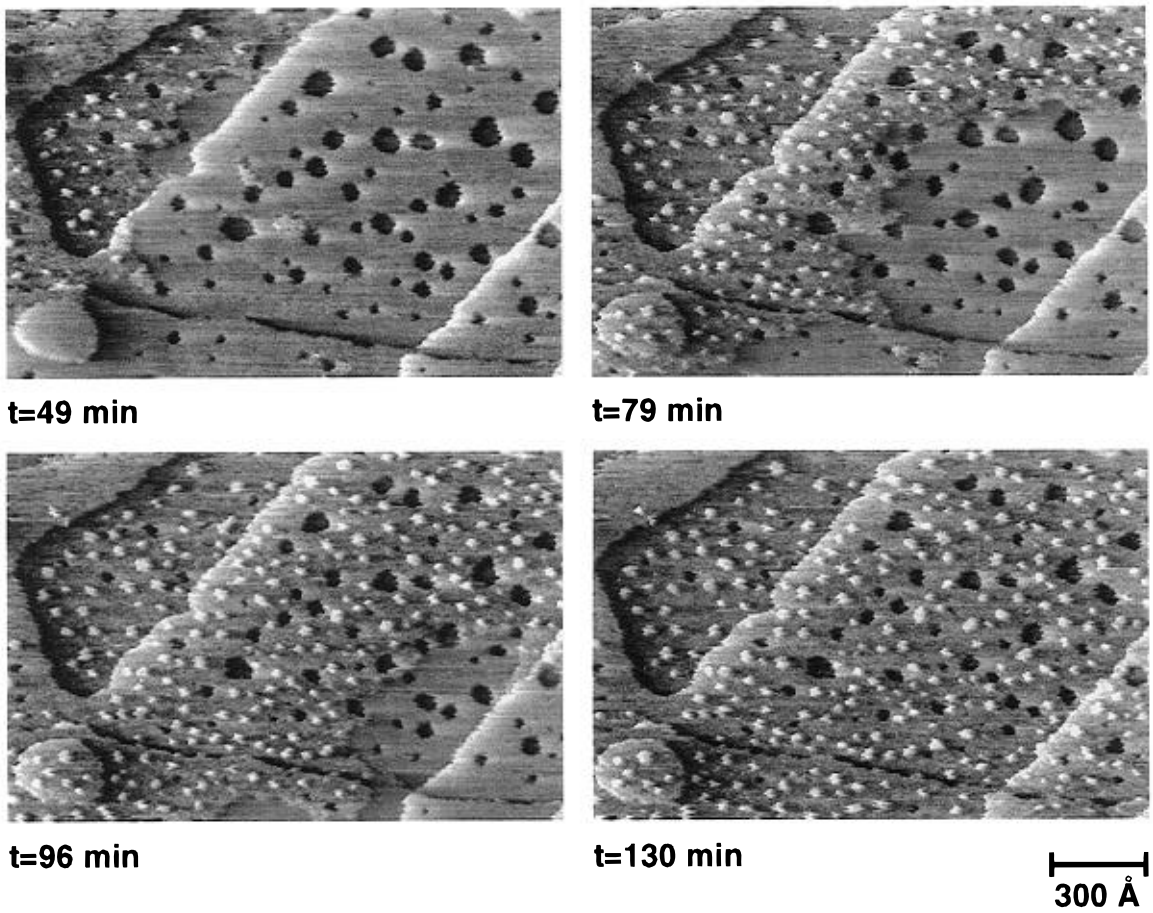

Figure 4. Image sequence of cluster growth on decanethiol covered Au(111) surface taken at +150 mV. Tunneling conditions: 0.6 nA, +50 mV tip bias.

of the surface remained unchanged since it had been established as early as +50 mV. In Figure 5b, the potential was stepped to −220 mV, and now bulk precipitates begin to form, as seen by the nucleation of a large nodule at the bottom of the image. The growth of this isolated deposit is followed in Figure 5b−d. The potential was held at −220 mV in Figure 5c and raised to −200 mV in Figure 5d, where despite this reversal, the nodule continued to grow. Thus, the growth of this nodule was evidently kinetically limited, perhaps by the close proximity of the tip, and it is not clear which was the exact threshold potential for the formation of bulk deposits. The growth sequence shown in Figure 5 was acquired over 30 min. However, further reversal of the potential caused dissolution of the deposit.

The small Cu clusters proved to have a tenacious character as they themselves resisted dissolution at more anodic potentials generally after being held at negative potentials for periods of several hours. A quite dramatic example of this is shown in Figure 6, where the image sequence is the same surface as that of Figure 5. Here, the images were taken at highly anodic potentials, +700 mV for Figure 6a, and +1100 mV for Figure 6b−d. At +700 mV, most of the clusters have dissolved, but several remain (Figure 6a). At +1100 mV, some still remain, despite the fact that the underlying gold substrate itself is undergoing oxidation, as seen by the formation of large holes or pits in the surface in Figure 6b. In the subsequent image (Figure 6c), taken at the same potential, corrosion of the surface has progressed, and now no clusters remain. However, a fairly high density of clusters is still present approximately 1 h after the anodic progression began in the vicinity around the original scan zone, which is now highly corroded, as seen by the zoom-out in Figure 6d. It should be mentioned that the potential of +1100 mV is well below the threshold at which gold oxidation is detected by cyclic voltammetry in H_2SO_4 electrolytes, formally ca. 1300 mV vs SCE.[34] It is clear that the tip had accelerated the oxidative processes that are only evidenced in the scan zone. We do not put forth an explanation for this process but will mention that Gao and Weaver[35] had also observed pitting of Au(111) by in situ electrochemical STM, which had been undoubtedly induced by the tip after the gold had been subjected to oxidation at relatively high potentials (up to ca. 1500 mV vs SCE). Also, erosion of Au in cyanide-containing solutions was found to be enhanced if the tip bias was even 50 mV positive of the sample.[33] In our case, the tip bias was +50 mV with respect to the sample. It is also known that the thiols themselves will oxidatively desorb at approximately +1300 mV vs SCE in acidic electrolytes,[36] which would of course contribute to the surface corrosion. Despite these destablilizing effects, the fact still remains that clusters are present at over 1000 mV positive of their thermodynamic oxidation potential, suggesting that they have been passivated. The nature of this presumed passivation is currently undergoing further study in our laboratory.

The electric blocking nature of self-assembled alkyl thiol layers on gold electrodes has been thoroughly investigated.[18−21] From these studies, it has become clear that blocking behavior improves with alkyl chain length. To our knowledge, however, only indifferent electrolytes or outer-sphere redox couples (i.e., $Ru(NH_3)_6^{2+/3+}$, $Fe(CN)_6^{4-/3-}$, $Fe(H2O)_6^{2+/3+}$) have been used as probes to understand the blocking behavior.[18−21] Direct Cu UPD onto octadecanethiol layers on Au(111) and subsequent ex-situ imaging of the deposits had been tried, but only as a means of imaging defects in *incomplete* thiol monolayers, assuming that UPD took place in pinholes and at other defect sites.[37] In that study, cluster formation had also resulted, with

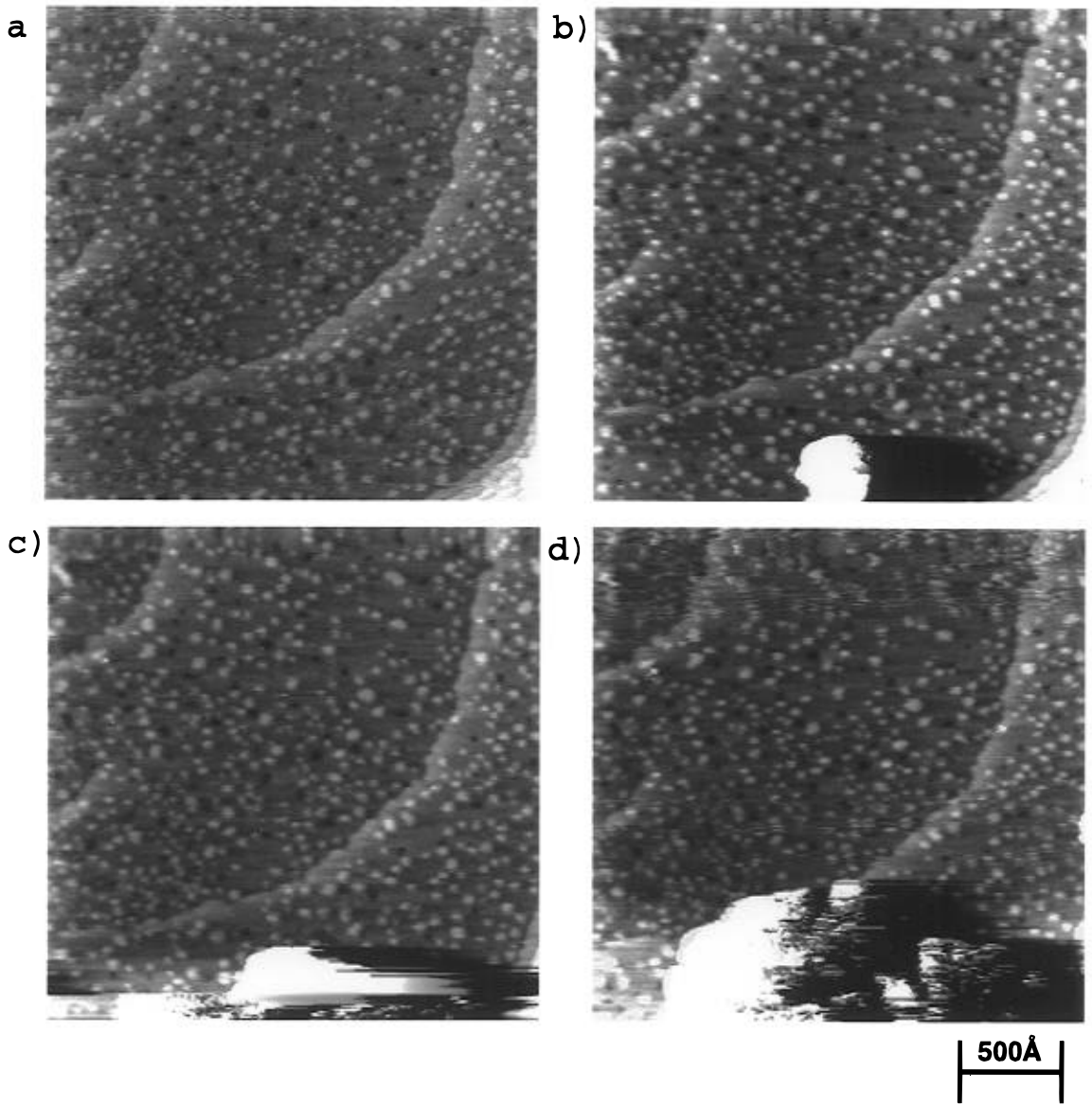

Figure 5. In situ image sequence on decanethiol-covered Au(111) in bulk deposition region, at point where bulk deposition begins. (a) −210, (b) −220, (c) −220, and (d) −200 mV (SCE). Bulk Cu nodule is seen growing at bottom of images. Note, however, Cu nanoparticle background experiences no change even at these very negative potentials. All images are 240 × 240 nm. Sequence acquisition time: 30 min. Tunneling conditions: 0.5 nA, +100 mV tip bias.

cluster density measured and claimed to decrease exponentially with thiol coverage measured by immersion time of the gold in the thiol solution. The cyclic voltammogram in Figure 1b for a decanethiol-covered electrode shows no peaks in the UPD region, and thus the deposition current is smaller than the double-layer charging current. We therefore claim that the deposition kinetics in the presence of a *complete* thiol monolayer must be too slow to permit observable currents to flow. In support of this, we take the deposition conditions during the acquisition of the images in Figure 4. The electrochemical current during this experiment was 50 nA at +150 mV. On the basis of this current, we estimate that approximately 20 min would be necessary to form 2/3 of a monolayer of Cu, assuming no hinderences.[38] However, the data of Figure 4 suggest that much more time is required to even form a full coverage of visible clusters. In addition, the surface coverage of the clusters has been measured to be about 10−15%. If one therefore assumes that 10−15% of the surface was exposed by pinholes and that Cu deposits directly into the pinholes of the thiol layer, then peaks or plateaus should be seen in the cyclic voltammogram, if the defect sites act as ultramicroelectrodes.[39] Our evidence shows that, for well-formed layers, no peaks are seen (cf. Figure 1b). From this evidence, as well as from the homogeneous nucleation seen with the STM, it is apparent that nanoparticles were not formed in pinholes or defects in the thiol layer. Penetration of Cu ions into the layer may be possible, but discharge of Cu^{+2} ions across the intervening alkane spacer layer by tunneling,[18] with subsequent diffusion and aggregation, is more likely to be the operative mechanism. This point is currently under investigation in our laboratory.

We should also mention that it is not possible to perform the cyclic voltammetry on the same electrode used for the STM measurements a priori. Doing so would leave a permanent cluster decoration at the outset of the STM experiments. Thus it is apparent that cluster deposition during dynamic scanning occurs at potentials near the negative extreme of the sweep. It should be mentioned at this point that cyclic voltammograms taken after the STM experiments showed the presence of peaks, indicating that the thiol layer had acquired a rather high density of defects induced by the electrochemistry.[37,39]

Another point which is open to further study is the finding that no further development had occurred after the initial cluster

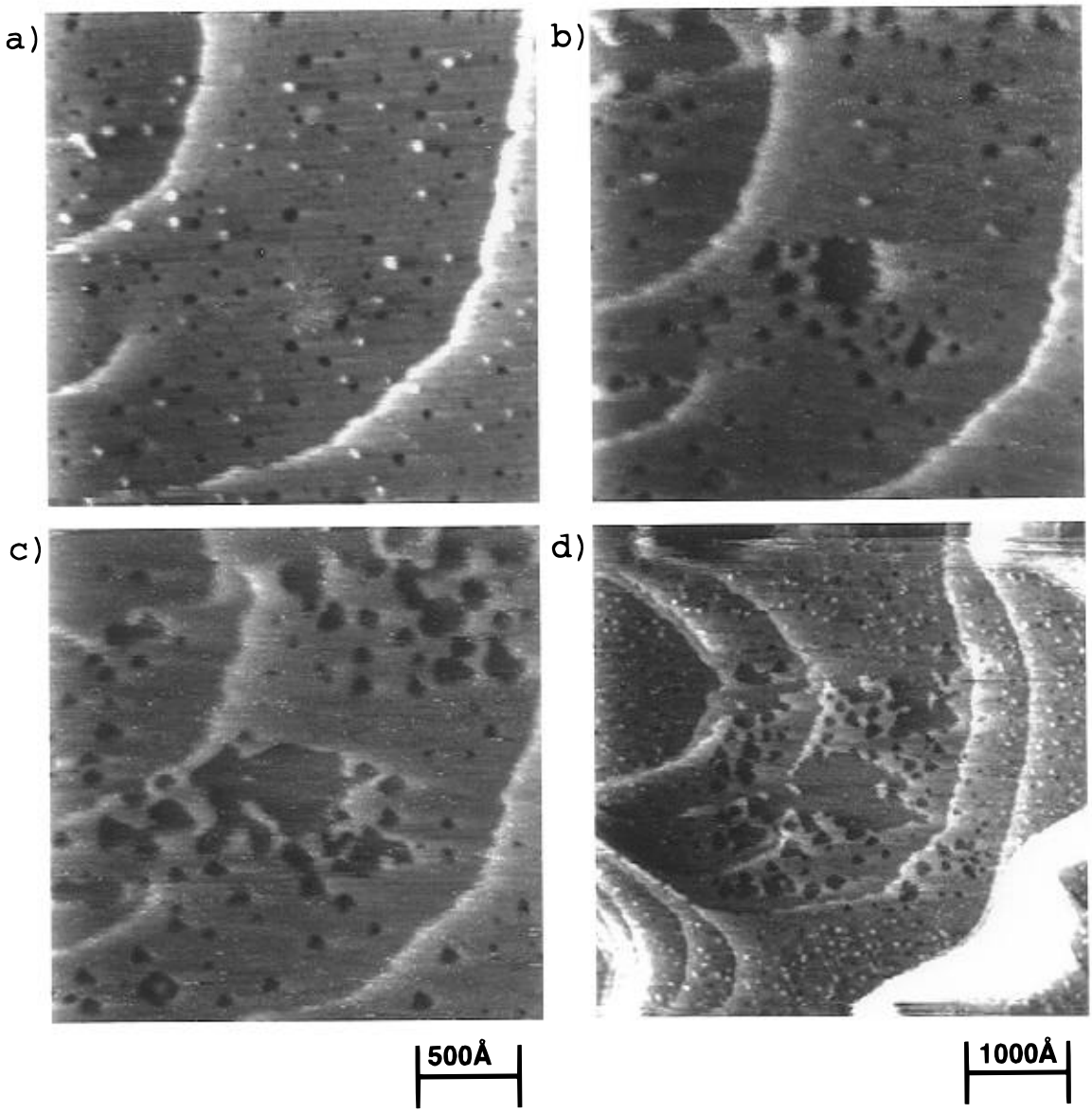

Figure 6. In situ image sequence on same surface shown in Figure 4, but at potentials near that of bulk oxidation of Au. (a) +700 mV, (b−d) +1100 mV. Progressive corrosion of Au surface is seen in images, with dissolution of Cu nanoparticles. Zoom-out shown in (d) shows that oxidative processes had only impacted on the region scanned by STM tip. All images are 240 × 240 nm. Sequence acquisition time: 1 h. Tunneling conditions: 0.5 nA, +80 mV tip bias.

growth. That is, that essentially all clusters had attained a maximum size at potentials in the UPD region and that no formation of bulk deposits was observed until potentials well into the bulk deposition zone were applied to the substrate. In addition, the clusters remain intact at potentials well positive of their dissolution potential. In other experiments, we had observed that even clusters on electrodes held at +600 mV for 12 h did not dissolve. As mentioned above, we are proposing that the clusters become passivated, perhaps being protected by thiol molecules that have somehow been displaced during Cu cluster formation. This type of exchange of the thiolate−metal bond is thought to occur with silver layers vacuum deposited on hexadecyl thiol layers. In that study, there is evidence by XPS that the thiol detaches from the Au substrate and rebonds with the Ag. At this juncture, it can be mentioned that Cu has also been vacuum deposited onto functionalized thiol layers (−OH,[41] −COOH,[42] and $COOCH_3$[43] headgroups). Spectroscopic studies on the first three sytems did indicate formation of Cu−O bonds between the Cu and the headgroup unit and indicated that low coverages of Cu (<0.5 nm), essentially little or no penetration into these functionalized thiol layers had occurred. Unfortunatley, no study on methyl terminated thiol layers has been reported.

Conclusion

In summary, we have followed the electrodeposition of Cu on decanethiol-covered Au(111) electrodes in situ with electrochemical STM. It was found that the Cu deposition proceeded as an instantaneous nucleation and growth of nanoparticles within the potential window known as the UPD region on bare gold electrodes. Nanoparticle creation was observed to start and finish within the UPD potential range. The deposition begins by nucleation and rapid growth of cluster patches, which apparently spreads and seeds the surface with clusters that nucleate at the advancing patch front. The cluster distribution takes on a homogeneous appearance. The measured clusters fell into a range between 2 and 5 nm in diameter, the average being 3 nm. The height was found to be 2−3 Å, corresponding to one atomic layer. Once the clusters have established themselves, no new nucleation of clusters is observed, nor do the clusters grow in size, as the potential is

made increasingly cathodic. In accordance with this growth mechanism, the cyclic voltammetry shows no current peaks in the UPD region, indicating that the deposition kinetics in the presence of the thiol layer are too slow to permit observation of any peaks above the background charging currents. These clusters nucleate on the flat portions of terraces and are not found to nucleate at step edges nor other morphological defects on the thiol-covered Au(111) surface, in contrast to growth of bulk Cu electrodeposits on bare gold found in earlier studies. At potentials close to 200 mV negative of the Nernstian potential, growth of isolated bulk nodules is observed. Moreover, the clusters do not dissolve even at potentials 1000 mV positive of the Nernstian potential.

Electrodeposition on self-assembed organic monolayers might provide a versatile route for the fabrication of nanometer-scale surface structures. It is particularly attractive as it introduces two independent control parameters: the electrochemical potential and the chemical nature of the thiol tail group. It is the tail functional group of the SAMs that dominates the interaction between the monolayer and the contacting electrolyte and thus is of importance for the cluster formation. We are currently exploring the influence of the chemical nature of the tail group on the electrodeposition process and performing systematic studies of growth kinetics.

Acknowledgment. We thank Dr. Albert Schulte for introducing us to the tip-coating technique. We are grateful to Dr. Richard Nichols for helpful discussions on the electrochemistry of Cu UPD on clean gold. This reseach has been supported by the Schweizerischer Nationalfonds.

References and Notes

(1) Bard, A. J.; Abruña, H. D.; Chidsey, C. E.; Faulkner, L. R.; Feldberg, S. W.; Itaya, K.; Majda, D.; Melroy, O.; Murray, R. W.; Porter, M. D.; Soriaga, M. P.; White, H. S. *J. Phys. Chem.* **1993**, *97*, 7147−7173 and references therein in conjunction with part IV of this review.

(2) Röder, H.; Hahn, E.; Brune, H.; Bucher, J.-P.; Kern, K. *Nature* **1993**, *336*, 143.

(3) Jung, D. R.; Czanderna, A. W. *Crit. Rev. Solid State Mater. Sci.* **1994**, *19*, 1 and references therein.

(4) Hachiya, T.; Honbo, H.; Itaya, K. *J. Electroanal. Chem.* **1991**, *3*, 275.

(5) Magnussen, O. M.; Hotlos, J.; Nichols, R. J.; Kolb, D. M.; Behm, R. J. *Phys. Rev. Lett.* **1990**, *64*, 2929.

(6) Magnussen, O. M.; Hotlos, J.; Beitel, G.; Kolb, D. M.; Behm, R. J. *J. Vac. Sci. Technol. B* **1991**, *9*, 969.

(7) Shi, Z. Lipowsi, J. *J. Electroanal. Chem.* **1994**, *365*, 303.

(8) Borges, G. L.; Kanazawa, K. K.; Gordon, J. G.; Ashley, K; Richer, J. *J. Electroanal. Chem.* **1994,** *364*, 281.

(9) Zei, M. S.; Qiao, G.; Lehmpfuhl, G.; Kolb, D. M. *Ber. Bunsen-Ges. Phys. Chem.* **1987,** *91*, 349.

(10) Shi, Z.; Lipkowski, J. *J. Electroanal. Chem.* **1994**, *364*, 289.

(11) Nichols, R. J.; Kolb, D. M.; Behm, R. J. *J. Electroanal. Chem.* **1991**, *313*, 109.

(12) Nichols, R. J.; Beckmann, W.; Meyer, H.; Batina, N.; Kolb, D. M. *J. Electroanal. Chem.* **1992**, *330*, 381.

(13) Haiss, W; Lackey, D.; Sass, J. K; Meyer, H.; Nichols, R. J. *Chem. Phys. Lett*, **1992**, *200*, 343.

(14) Wünsche, M.; Nichols, R. J.; Schumacher, R.; Beckmann, W. Meyer, H. *Electrochim. Acta* **1993**, *38*, 647.

(15) Dakkouri, A. S.; Batina, N.; Kolb, D. M. *Electrochim. Acta* **1993**, *38*, 2467.

(16) Bucher, J.-P.; Röder, H.; Kern, K. *Surf. Sci*. **1993**, *289*, 370.

(17) Schulte, A. Ph.D. Dissertation 1994, Department of Inorganic Chemistry, University of Münster. Bach, C. E.; Nichols, R. J.; Beckmann, W.; Meyer, H.; Schulte A.; Besenhard, J. O.; Jannakoudakis, P. D. *J. Electrochem. Soc.* **1993**, *140*, 1281−1284. (Note: the product quoted in the latter reference is no longer produced by BASF and has been replaced by that quoted in text herein.)

(18) Porter, M. D.; Bright, T. B.; Allara, D. L.; Chidsey, C. E. D. *J. Am. Chem. Soc.* **1987**, *109*, 3559.

(19) Sondag-Heuthorst, J. A:M.; Fokkink, L..G. J. *J. Electroanal. Chem.* **1994**, *367*, 49.

(20) Sondag-Heuthorst, J. A. M.; Fokkink, L. G. J.*Langmuir* **1995**, *11*, 2237.

(21) Chidsey, C. E. D.; Loiacono, D. N. *Langmuir* **1990**, *6*, 682.

(22) Toney, M. J.; Howard, J. N.; Richer, J.; Borges, G. L.; Gordon, J. G.; Melroy, O.R. *Phys. Rev. Lett.* **1995,** *75*, 4472.

(23) Huckaby, D. A.; Blum, L. *J. Electroanal. Chem*. **1991**, *315*, 255.

(24) Höltze, M. H.; Retter, U.; Kolb, D. M.; *J. Electroanal. Chem*. **1991**, *371*, 101.

(25) Haiss, W.; Sass, J. K.; Lackey, D.; van Heel, M. Analysis and Interpretation of Scanning Tunneling Microscopy in an Electrochemical Environment: Copper on Au(111). In *Atomic Force Microscopy/Scanning Tunneling Microscopy*; Cohen, S. H., et al., Eds.; Plenum: New York, 1994; p 423.

(26) Melroy, O. R.; Samant, M. G.; Borges, G. L.; Gordon II, J. G.; Blum, L.; White, J. H.; Albarelli, M. J., McMillan, M.; Abruña, H. D. *Langmuir* **1988**, *4*, 728.

(27) Bucher, J.-P.; Santessen, L.; Kern, K. *Appl. Phys. A* **1994**, *59*, 135−138; *Langmuir* **1994**, *10*, 979.

(28) McDermott, C. A.; McDermott, M. T.; Green, J.-B.; Porter, M. D. *J. Phys. Chem*. **1995**, *99*, 13257.

(29) Sondag-Huethorst, J. A. M.; Schöenenberger, C.; Fokkink, L. G. J. *J. Phys. Chem*. **1994**, *98*, 6826.

(30) Chailapakul, O.; Sun, L.; Xu, C.; Crooks, R. M. *J. Am. Chem. Soc*. **1993**, *115*, 12459.

(31) Schöenenberger,C.; Sondag-Huethorst, J. A. M.; Jorritsam, J.; Fokkink, L. G. J. *Langmuir* **1994**, *10*, 611.

(32) Cavalleri, O; Hirstein, A.; Kern, K. *Surf. Sci. Lett*. **1995**, *340*, L960.

(33) Li, Y.-Q.; Chailapakul, O.; Crooks, R. M. *J. Vac. Sci. Technol. B* **1993**, *13*, 1300.

(34) Angerstein-Kozlowska, H.; Conway, B. E.; Hamlin, A.; Stoicoviciu, L. *J. Electroanal. Chem*. **1987**, *228*, 429.

(35) Gao, X.; Weaver, M. J. *J. Electroanal. Chem*. **1994**, *267*, 259.

(36) Widrig, C. A.; Chung, C.; Porter, M. C. *J. Electroanal. Chem.* **1991**, *310*, 331.

(37) Sun, L.; Crooks, R. M. *J. Electrochem. Soc*. **1991**, *138*, L23.

(38) Electrode area 0.2 cm^2, 0.44 mC/cm^2 required to deposit complete Cu (1 × 1) monolayer (see refs 4 and 33).

(39) Amatore, C.; Savéant, J.-M.; Tessier, D. *J. Electroanal. Chem.* **1983**, *147*, 39. Chailapakul, O.; Crooks, R. M. *Langmuir* **1993**, *9*, 884.

(40) Tarlov, M. J. *Langmuir* **1992**, *8*, 80.

(41) Jung, D. R.; King, D. E.; Czanderna, A. W. *Appl. Surf. Sci*. **1993**, *70/71*, 127.

(42) Czanderna, A. W.; King, D. E.; Spaulding, D. *J. Vac. Sci. Technol. A* **1991**, *9*, 2607. Smith, E. L.; Alves, C. A.; Anderegg, J. W.; Porter, M. D.; Siperko, L. M. *Langmuir* **1992** *8*, 2707.

(43) Allara, D. L.; Jung, D. R.; Zhang, P. Metal Atom Reactions with Self-Assembled Monolayers Studied by In-Situ IR Vibrational and X-Ray Photoelectron Core Level Spectroscopy. Paper presented at 39th Natl. Symp. American Vacuum Society, Chicago, Nov 9−13, 1992 (unpublished). See also ref 3.

JP960053W